



# Impact of Sisal Fiber Reinforcement on the Mechanical and Physical Properties of One-Part Geopolymer Mortar with a Ternary Binder System

Enchapparackal Subash Poojalakshmi\*, Praveen Nagarajan, Janardhanan Sudhakumar and Blessen Skariah Thomas  
Department of Civil Engineering, National Institute of Technology Calicut, Kerala, India

Sreelakshmi Mughavan Kandi and Anupriya Thekke Maveettil  
Department of Civil Engineering, Government Engineering College Calicut, West Hill, India

\* Corresponding author. E-mail: poojalakshmi1@gmail.com DOI: 10.14416/j.asep.2025.07.002  
Received: 9 February 2025; Revised: 29 April 2025; Accepted: 26 May 2025; Published online: 2 July 2025  
© 2025 King Mongkut's University of Technology North Bangkok. All Rights Reserved.

## Abstract

This study investigates the influence of chemical treatment and fiber content on the mechanical and durability properties of sisal fiber-reinforced one-part geopolymer mortar (OP-GPM) incorporating a ternary binder system of diatomite, feldspar, and ground granulated blast furnace slag (GGBS). Sisal fibers were treated with 0.5%, 5%, and 10% NaOH solutions for 2 and 24 h and incorporated at 0.5–2% by binder weight. The workability, compressive strength (CS), flexural strength (FS), split tensile strength (STS), ultrasonic pulse velocity (UPV), water absorption, and chemical resistance were evaluated. Optimal performance was achieved with 1% fiber content and fibers treated with 5% NaOH for 2 h, leading to a 15% increase in CS (54 MPa) and notable improvements in FS (8.62 MPa) and STS (5.88 MPa). Alkali treatment significantly enhanced fiber crystallinity and tensile strength, with a 208% reduction in fiber water absorption. However, excessive fiber content (>1%) reduced workability and mechanical performance. Regression analysis showed strong correlations between the strength properties. The study confirms that properly treated sisal fibers improve the mechanical and durability performance of OP-GPM, offering a sustainable alternative to conventional reinforcement in geopolymer composites.

**Keywords:** Diatomite, Feldspar, Ground granulated blast furnace slag, One-part geopolymer, Sisal fiber

## 1 Introduction

The expanding need for infrastructure development has resulted in a surge in the requirement for Portland cement, a major source of greenhouse gas emissions. India accounts for almost 8% of the global cement production capacity, positioning it as the second-largest cement producer globally, following China. India contains many places with potentially substantial amounts of limestone, which is important for the manufacture of cement. About 2.8 tonnes of ingredients, comprising fuel as well as additional resources, are required to make one tonne of Portland cement, which also produces 5–10% of dust. Each tonne of one-part geopolymer emits 1 tonne of CO<sub>2</sub> [1], [2]. By 2025, the cement sector in India is anticipated to grow by about 80 million tonnes. Many

alternatives are being developed by experts in an effort to lessen the dependency on Portland cement. Geopolymers (GP) are one of them, which uses zero cement. A French scientist Joseph Davidovits coined the term “geopolymer”. It is an effective process that creates a hard mass by using raw materials comprised of silica and alumina in combination with an activator [3]. Commonly employed raw materials include fly ash, GGBS, metakaolin, rice husk ash, and others. A multitude of work has been done to evaluate the effectiveness of GPs that use different types of binders [4]–[6]. The majority of the research's conclusions supported the usage of GP as a Portland cement substitute in construction [7]–[10]. It provides a desirable alternative for conventional industrial uses in which a significant amount of garbage must be stabilised [11].



Despite being a good substitute, its quick setting time, requirement for high temperatures to cure, absence of appropriate standards, use of hazardous chemicals, etc., prevent it from being utilized extensively as a cementitious material. The main challenge in the practical application of GP lies in the use of harmful chemical solutions [12]. Consequently, researchers are currently directing their attention towards one-part GP, a substance that can be created simply by adding water, similar to cement concrete. Nevertheless, the tensile strength and FS of these materials are low [13]. Thus, one technique to improve the strength is fiber reinforcement. Different varieties of fibers, including synthetic and natural fibers, can be employed to enhance the TS of cement-based materials [14]–[18]. Natural fibers have been increasingly investigated as eco-friendly reinforcement materials in cementitious and geopolymeric composites, primarily due to their renewability, biodegradability, and capacity to enhance tensile and flexural properties through crack-bridging mechanisms. Among the various natural fibers, sisal fiber has gained attention for its high tensile strength, moderate modulus of elasticity, and good compatibility with alkaline matrices [19], [20].

The effectiveness of fiber reinforcement in a brittle matrix such as geopolymer mortar depends on several factors, including fiber type, content, orientation, and notably, fiber length. Fiber length plays a critical role in determining the quality of stress transfer across the fiber-matrix interface, which directly impacts mechanical performance. If the fibers are too short, they may not provide sufficient bridging across cracks; conversely, excessively long fibers are prone to entanglement, non-uniform dispersion, and reduction in workability [21]. Therefore, an optimal fiber length is essential to ensure a balance between mechanical enhancement and mix processability. Several studies have reported favorable results using short sisal fibers in the range of 10 to 20 mm. Onuaguluchi and Banthia emphasized that natural fibers within this length range contributed effectively to energy dissipation and enhanced post-cracking ductility in cement-based materials without severely compromising workability [22]. Similarly, Toledo Filho *et al.*, found that 10 mm sisal fibers exhibited improved durability and homogeneity in composite mixtures, compared to longer fibers, which often induced mixing difficulties and voids due to clustering [23]. In geopolymer-based systems, Savastano *et al.*, demonstrated that sisal fibers with 10 mm length,

when uniformly dispersed, enhanced both compressive and flexural strength by improving microcrack resistance and increasing energy absorption capacity. They also noted that longer fibers posed difficulties in mixing and uniform distribution due to the inherently viscous nature of geopolymer pastes [24].

Based on these findings, the current study adopts a sisal fiber length of 1 cm, which falls within the range demonstrated to be effective for mechanical reinforcement in cementitious and geopolymeric systems. This choice is further supported by preliminary trials conducted during this research, where longer fiber lengths resulted in poor dispersion, reduced workability, and visible fiber clumping, undermining the consistency and structural integrity of the mix.

However, using natural fibers can also come with its own set of problems, like fiber deterioration [25]. Various techniques are adopted to prevent the deterioration of natural fibers. It has been discovered that treating natural fibers with alkali effectively stops them from degrading [26], [27]. Wei and Meyer observed that decreasing the alkalinity of the pore solution can help slow down the deterioration of fibers [28]. Edeerozey *et al.*, discovered that alkali treatment greatly enhanced the mechanical characteristics of kenaf fibers [29]. The benefits of alkali treatment for natural fiber composites were emphasised by Sahu *et al.*, [30] and Narayana *et al.*, [31]. These benefits included higher water absorption resistance, stronger adhesion with polymers, and increased strength. Alkali treatment is a potential technique for maintaining the integrity of natural fibers, according to the aggregate findings of these investigations.

The effectiveness of alkali treatment is highly dependent on the concentration of NaOH used. Mwaikambo and Mwaikambo and Ansell reported that low concentrations (typically <1%) may result in insufficient surface modification, while excessively high concentrations (>10%) can lead to pronounced fiber degradation, including excessive delignification and weakening of mechanical integrity [32].

Optimal concentrations generally lie in the range of 3% to 7%, where improved mechanical interlocking and moderate defibrillation occur without compromising fiber strength [33], [34]. In this context, the present study adopts three strategically selected NaOH concentrations: 0.5%, 5%, and 10%, representing a mild, moderate, and aggressive level of chemical modification. The 0.5% level was chosen to

explore the minimal threshold for surface cleaning without significantly altering fiber morphology. The 5% level represents an intermediate value frequently reported in literature to yield enhanced fiber–matrix interaction with minimal structural compromise. Finally, 10% was selected to study the upper limit of fiber tolerance to alkali treatment, where significant surface roughening and possible structural breakdown are expected. This tri-level approach facilitates a comprehensive understanding of how varying alkali intensities influence the mechanical, microstructural, and durability behavior of geopolymer mortar reinforced with natural fibers.

The efficiency of alkali treatment is influenced not only by NaOH concentration but also by the treatment duration. Short treatment times may only partially clean the fiber surface, whereas extended durations can lead to more profound structural changes, including partial defibrillation or degradation of fiber integrity [35], [36]. Thus, selecting treatment times that represent both moderate and extended exposure is critical for understanding the balance between surface modification and potential fiber weakening.

In this study, treatment durations of 2 h and 24 h were selected to represent two distinct regimes of fiber modification: a moderate short-term treatment (2 h) aimed at removing surface impurities and enhancing fiber roughness, and a long-term treatment (24 h) intended to investigate the extent to which deeper chemical alterations affect fiber performance and matrix interaction. This dual-time selection is consistent with literature ranges where alkaline treatment durations vary widely, from 30 min to 48 h, depending on fiber type, NaOH concentration, and target application [37], [38]. For instance, Mwaikambo and Ansell reported significant changes in sisal fiber morphology and mechanical performance between 1 h and 24 h treatments using NaOH, highlighting the critical effect of treatment duration [32]. Also, the preliminary analysis on short-term treatment was conducted for 1, 2, and 3 h, in which the optimum fiber modifications were observed for 2-hour treatment. Hence, this study fixed 2 h as the short-term treatment and 24 h as the long-term treatment.

The present study examines the impact of alkali treatment and fiber content on the characteristics of sisal fiber-reinforced OP-GPM. The precursor consisted of a mixture of diatomite, feldspar, and GGBS. Diatomite powder is a finely milled material obtained from the long-preserved remnants of diatoms, which are microscopic unicellular algae in

water. Diatoms gradually collect in the sediment of rivers, lakes, and seas. The powder consists of 80–90% silica, which is a naturally occurring material present in several organisms, including plants and people. Studies on GP utilizing diatomite have demonstrated encouraging outcomes. A research done by Ilkentarap *et al.*, found that the incorporation of diatomite to GP mortars significantly improved their flexural and CS, as well as their abrasion resistance [39]. The progress of the microstructure and strength properties of GP pastes was observed by Santos *et al.*, with the incorporation of diatomite [40]. Kipsanai *et al.*, highlighted the capacity of diatomaceous earth, a variant of diatomite, to produce eco-friendly and lightweight construction materials [41]. Feldspar is a collective term for a category of crystalline minerals composed of aluminium silicates combined with potassium, sodium, calcium, or barium. These minerals are abundant in rock formations and are the primary constituents of prominent rock varieties such as granites and gabbros. Being a siliceous material, feldspar has the potential to act as a binder in GP. It has been observed that geopolymers derived from feldspar, specifically albite and anorthite, demonstrate notable characteristics such as elevated CS and fire resistance [42], [43]. GGBS, commonly referred to as slag cement, is a residual material received as a byproduct in the process of iron production within blast furnaces. Due to its pozzolanic and hydraulic qualities, it is a highly valued supplemental cementitious material that plays a crucial role in sustainable construction methods [44]. The oxide composition of GGBS exhibits variability contingent upon the origin of the slag, although it generally comprises silicates, aluminates, and several other minor elements. The main constituents of GGBS consist of silica ( $\text{SiO}_2$ ), alumina ( $\text{Al}_2\text{O}_3$ ), and lime ( $\text{CaO}$ ), in addition to lesser quantities of magnesium oxide ( $\text{MgO}$ ), iron oxide ( $\text{Fe}_2\text{O}_3$ ), and various impurities. The reactivity and performance of GGBS in concrete mixtures are influenced by the amounts of these ingredients. GGBS serves as the primary substance in GPC, where it undertakes a chemical reaction with an activator solution to create a 3D network of aluminosilicate gel. The presence of a gel matrix in the concrete mixture serves to enhance binding and cohesion, comparable to the role of CSH gel in concrete made with Portland cement. Studies on GP composed of GGBS have demonstrated encouraging outcomes. As per the work conducted by Lavanya *et al.*, an elevated amount of GGBS in

geopolymer bricks resulted in enhanced CS and improved characteristics [45]. In the same vein, Saludung *et al.*, found that the CS of GP paste exhibited an upward trend as the quantity of GGBS increased [46]. The work done by El-Hassan *et al.*, delved deeper into the effect of process factors on the functionality of GP composites blended with fly ash and GGBS. The outcomes revealed that the final product may be improved by employing particular curing processes [47]. Rao *et al.*, examined the utilization of GGBS in GPC by including steel fibers, resulting in a notable improvement in the mechanical characteristics [48]. These investigations indicate that GGBS has the ability to serve as a crucial component in producing high-performance GP materials.

This study addresses a significant research gap regarding the impact of sisal fiber reinforcement on the structural development and properties of one-part GPs. The results shared here clarify how sisal fibers impact the mechanical properties and structure of this eco-friendly building material. By incorporating natural fibers, the research contributes to reducing the reliance on Portland cement, thus promoting both sustainability and enhanced performance of one-part GPs. Additionally, the type and volume fraction of natural fibers were found to significantly affect the strength and internal structure properties of the GP. The innovation of this study lies in creating new formulations that take into account the relationship between the amount of dispersed sisal fibers and the properties of one-part GPs derived from diatomite, feldspar, and GGBS. This approach offers a promising pathway to reducing the ecological effects of building materials, aligning with the broader goal of sustainable building practices.

## 2 Materials and methods

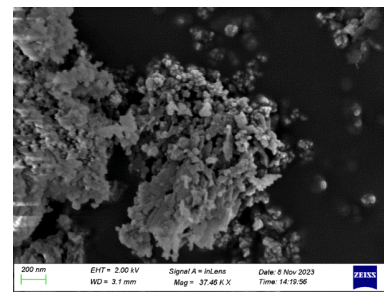
### 2.1 Precursor characterizations

In this work, a combination of diatomite, feldspar and GGBS plays the role of binder. Diatomite was procured from Haritson Minitech Pvt Ltd, Jaipur, India. Shri Giriraj Mineral, Rajasthan, India, provided the feldspar. GGBS was obtained from JSW cement, Calicut, Kerala. Diatomite is distinguished by its substantial amount of silica, usually more than 80%, and low density. It is frequently finely powdered and utilized in a variety of industrial applications, including filtration, adsorbents, abrasives, and as a part of brick and concrete compositions [49]–[55].

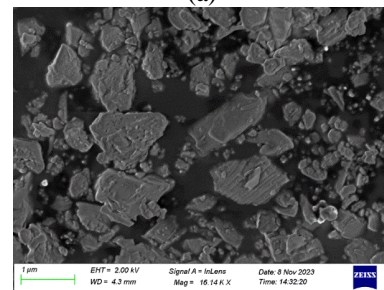
The diatomite used in this work contains 88% silica and 6% alumina. Feldspar, which is a rock forming mineral, was used as an additional source of alumina and it contained 61.19% silica and 15.12% alumina. GGBS contained 34% SiO<sub>2</sub>, 17% Al<sub>2</sub>O<sub>3</sub> and 37% CaO. Table 1 denotes the chemical composition and Figure 1 depicts the SEM image of the raw materials. Diatomite's microstructure primarily consists of plate-shaped diatoms. Some particles were rod-shaped, possibly indicating the presence of aluminosilicate and organic remnants [56].

**Table 1:** Oxides present in raw materials.

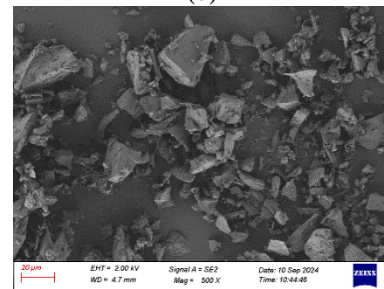
Element	Chemical Composition (%)					
	SiO <sub>2</sub>	Al <sub>2</sub> O <sub>3</sub>	Fe <sub>2</sub> O <sub>3</sub>	CaO	Na <sub>2</sub> O	K <sub>2</sub> O
Diatomite	88	6	1	1.5	-	-
Feldspar	61.19	15.12	0.7	3.5	9.2	8.6
GGBS	34	17	0.6	37	-	-



(a)



(b)



(c)

**Figure 1:** SEM image of a) diatomite b) feldspar c) GGBS.

## 2.2 Aggregate

The mortar was made using fine aggregate composed of M sand particles with sizes less than 4.75 mm. Figure 2 displays the particle size distribution of fine aggregate, while Table 2 presents the parameters of fine aggregate. The aggregate is classified under zone II.

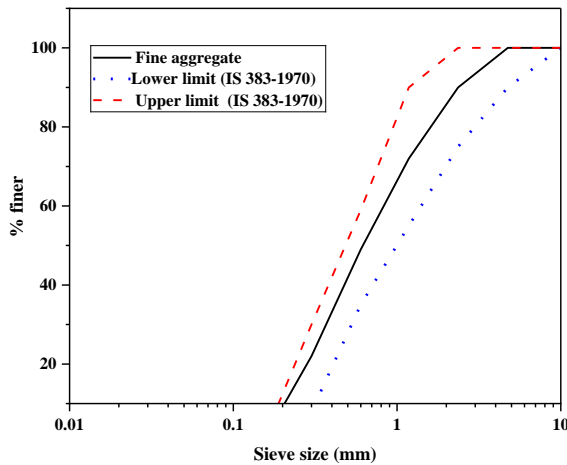


Figure 2: Particle size distribution of fine aggregate.

Table 2: Specifications of fine aggregate.

Parameter	Result
Water absorption	0.7%
Fineness modulus	2.5
Specific gravity	2.56
Bulk density	1.7 kg/l

## 2.3 Activator

The activators employed in the development of the one-part GP mix consisted of commercially available sodium hydroxide (NH) with a purity level of 98% and sodium silicate (SS). Based on prior experiments, the concentration of activator was established at 10% by weight of the binder, while the ratio of SS/NH was determined to be 1.5.

## 2.4 Fiber preparation

Sisal fiber obtained from the Eco green unit, Coimbatore was used as the reinforcing material. The fibers underwent a rigorous washing process using distilled water to eliminate any contaminants. After that, it is dried in sunlight and combed to make it

isolated and straight. The adopted fiber length was 1 cm and the fiber contents adopted were 0.5%, 1%, 1.5%, and 2% by weight of binder. Figure 3 shows the raw sisal fiber.



Figure 3: Raw sisal fiber.

## 2.5 Fiber treatment

The fiber was treated by immersing it in NH solutions with concentrations of 0.5, 5, and 10% for durations of 2 h and 24 h. By selecting 2 h and 24 h durations, we intended to explore both early-stage and late-stage modifications, thereby capturing the influence of alkali exposure on fiber-matrix compatibility across a meaningful range of structural transformation. The treated fibers were then washed with purified water to eliminate any remaining NH and were kept in an oven set to 70 degrees for 24 hours. Table 3 displays the treatment done for fiber. Figures 4 and 5 depict the fiber having a 1 cm length and fiber treatment, respectively.

Table 3: Parameters for fiber treatment.

Sl No	Treatment Time (h)	NH percentage
1	2	0.5
		5
		10
2	24	0.5
		5
		10



Figure 4: Fiber with 1 cm length.



**Figure 5:** Treatment of fiber.

## 2.6 Mixture preparation

Based on some trials, the ratio of diatomite, feldspar, and GGBS was fixed at 70:10:20. To make diatomite more reactive, it was calcined at 600 °C for two hours in a muffle furnace. Water-cement ratio was maintained at 0.45. Activator dosage was maintained as 10% by weight of binder and the ratio of SS/NH was taken as 1.5. The ratio of aggregate to binder was kept at 3. The precursors, sand, fiber, and activators were combined in a mortar mixer for 3 min to achieve a consistent blend. The superplasticizer and water were then added and mixed for at least 3 min until a consistent paste was achieved. The fresh paste was used to check the workability of the mix. Figure 6 represents the methodology for mortar preparation.

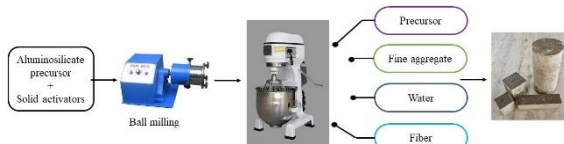


**Figure 6:** Mixing of one-part geopolymer.

## 2.7 Analysis of sample's properties

### 2.7.1 Water absorption

In order to obtain a uniform weight, 3 g of both treated and untreated fibers were collected and dehydrated in an oven at 80 °C for 24 h. Afterward, the fibers were allowed to remain at room temperature for 24 hours in distilled water. After taking the samples out of the water, they were wiped to remove any excess moisture and the final weight was noted. Equation (1) was employed to determine the water absorption capacity of fibers.

$$W_a (\%) = \frac{(w_1 - w_2)}{w_2} \times 100 \quad (1)$$

Where,  $W_a$  is the water absorption in percentage,  $W_1$  is the wet weight and  $W_2$  is the dry weight.

### 2.7.2 Tensile strength

The tensile strength test was done on a single strand fiber using a UTM. All specimens were maintained at a uniform length of 80 mm. The test was done in compliance with ASTM C 1557 [57]. A fiber is removed haphazardly from a bundle. Subsequently, the fiber was affixed in a testing apparatus and subjected to a load of 10 kg at a speed of 3.5 mm/min. The tensile strength was obtained by dividing the largest recorded force by the cross-sectional area perpendicular to the fiber axis at the fracture point. The Young's modulus was calculated by fitting a straight line to the linear segment of the stress-strain curve acquired during the tensile test. Figure 7 displays the arrangement for measuring tensile strength.

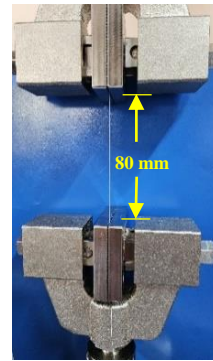


**Figure 7:** Tensile strength test of fiber.

### 2.7.3 X Ray Diffraction (XRD)

The variations in the crystallinity of fibers in response to treatment were determined through the utilization of XRD investigation. A Bruker Kappa Apex II X-ray diffractometer was utilized to measure the XRD patterns. The patterns were conducted using Ni filtered copper radiation with a 40 mA of current and 45 kV of voltage. Both treated and untreated fibers were analyzed. The scanning range was between 0 and 90 degrees. The crystallinity index was determined following Segal's approach [58]. The intensity values of the greatest and lowest peaks were utilized to determine the crystallinity index. Equation 2 was used for finding the crystallinity index.

$$I = \frac{I_{cr} - I_{am}}{I_{cr}} \times 100 \quad (2)$$

Where,  $I$  is the crystallinity index in percentage,  $I_{cr}$  corresponds to the intensity of the highest peak and  $I_{am}$  denotes the intensity of the lowest peak.

#### 2.7.4 Scanning Electron Microscopy (SEM)

SEM was employed to evaluate the influence of alkali treatment on the microstructure of the fiber. The ZEISS Sigma microscope was used to analyze the microstructure. Analysis was performed on both treated and untreated fibers.

### 2.8 Workability test

Workability of mortar with and without fiber was assessed using a flow table test as per ASTM C 1437-15 [59]. The flow table was thoroughly cleansed, and a flow mould was positioned precisely at the center. After filling the mould, the flow table was dropped 25 times and the flow diameter was measured.

### 2.9 Compressive, flexural and split tensile strength

The test was done in line with the guidelines of ASTM C 109 [60].  $50 \times 50 \times 50$  mm cubes were fabricated and subjected to testing at a loading rate of 0.58 kN/s. The specimens in this experiment were positioned utilizing the Universal Testing Machine (UTM), which can withstand stresses of up to 200 kilonewtons (kN). The CS is defined as the ratio of the failure load to the specimen's area. Figure 8(a) depicts the experimental configuration employed for quantifying CS.

Composite materials such as concrete and mortar exhibit unique characteristics when exposed to tension and compression. They have strong CS and poor tensile strength. FS test was conducted following the ASTM C 348 standard [61]. Mortar specimens were created with a binder to sand ratio of 1:3. The experiment was carried out using prisms with a  $40 \text{ mm} \times 40 \text{ mm} \times 160 \text{ mm}$  configuration and tested at a speed of 0.05 kN/s. The specimens were loaded using center point loading. Figure 8(b) displays the experimental arrangement. The STS test was performed as per ASTM C 496 [62].  $100 \times 200$  mm cylinders were used. The loading rate was 1.83 kN/s. The test configuration is shown in Figure 8(c).



(a)



(b)



(c)

**Figure 8:** (a) Compressive, (b) Flexural and (c) Split tensile strength tests.

### 2.10 Durability tests

#### 2.10.1 Ultrasonic pulse velocity

UPV is a non-invasive technique employed to assess the quality, safety, and uniformity of concrete



structures. The methodology involves the transmission of high-frequency ultrasonic pulses into the concrete, followed by the measurement of the duration it takes for the pulses to propagate through the material. The test was executed based on ASTM C 597 [63]. The pulse velocity was measured through direct transmission of ultrasonic waves through 50mm cube specimens.

### 2.10.2 Water absorption

The measurement of water absorption in the mortar sample was conducted using the guidelines provided in ASTM C 642 [64]. 50 mm cubes were placed in an oven and dried at a temperature between 100 and 110 degrees for 24 h, until they reached a stable weight. After 24 h, the samples were taken out of the oven and left to cool to room temperature. The initial weight of the specimens was observed and documented. Following the processes of drying, cooling, and weighing, the samples were kept in water for 48 h. The samples were extracted from the aqueous medium and desiccated by gently removing any surplus moisture using a dry cloth. The final weight of the specimen was subsequently recorded, and the associated water absorption was subjected to calculation.

### 2.10.3 Acid resistance

The test for acid resistance was carried out based on the ASTM C 1898 [65]. After a 28-day curing period, the specimens were subjected to a 24-h drying process and were then weighed to assess their initial weight. The cubes were dipped in a 5% HCl solution that had been diluted to a pH of 2, and left to soak for a duration of 56 days. The concentration of the solution was checked on a weekly basis. Following a period of 56 days, the cubes were extracted. Thoroughly removed any unstable particles that were released from the acid, measured in weight, and then tested for compression. The percentage reduction in weight and strength is determined by utilising the initial and final weights, in conjunction with CS data.

### 2.10.4 Sulphate resistance

Sulphate resistance test was performed following the guidelines provided in ASTM C267-20 [66]. The specimens' initial weight was measured following a curing period of 28 days and a drying period of 24 h.

The samples were then submerged in a solution containing 5% magnesium sulphate for a duration of 56 days. The weight change and CS were tested after 56 days.

## 3 Results and Discussions

### 3.1 Water absorption of fiber

The data presented in Table 4 illustrate the outcomes of water absorption in fibers exposed to various alkali concentrations and durations. The values were in the range of 31 to 95.78%.

**Table 4:** Water absorption of fiber.

NH %	Treatment Time (h)	Water Absorption (%)
0.5	2	83
0.5	24	75
5	2	68
5	24	55
10	2	40
10	24	31
Raw	--	95.78

When fibers were treated with 0.5% NH for 2 h and 24 h, they absorbed 83% and 75% of water, respectively. Fibers treated with 5% NH absorbed 68% and 55% of water after 2 h and 24 h, respectively. The application of a 10% concentration of NH caused a drop-in water absorption ability of sisal fibers in comparison to fibers treated with concentrations of 0.5% and 5% NH. Fibers exposed to 10% NH for 2 hours and 24 hours showed absorption rates of 40% and 31%, respectively. The water absorption of raw fiber was 95.78%. From the results, it is noticeable that alkali treatment decreased the water absorption of fibers. 10% NH-treated fiber for 24 h resulted in the lowest water absorption. It caused a 208% reduction in water absorption than the untreated fibers. Alkali treatment made the fiber hydrophobic by eliminating hydrophilic components like hemicellulose and lignin. This significantly reduces the affinity of fiber for water. In addition, alkali treatment can result in an enhancement of the crystallinity of cellulose, which is the main constituent of sisal fiber. Increased crystallinity decreases the ability of water molecules to reach the interior structure of the fiber, resulting in reduced water absorption [67].

### 3.2 Tensile strength of fiber

Table 5 shows the result of the tensile strength, percentage elongation and Young's modulus of single-stranded fiber subjected to various NH concentrations and times.

The application of a 0.5% NH treatment to the fiber for 2 h yielded the greatest TS and Young's modulus. But its elongation percentage was slightly less than the one treated with 0.5% NH for 24 h. When compared with the raw fiber, sisal fiber treated with 0.5% for 2 h resulted in an increase of 93.22, 230, 1.34% in TS, Young's modulus and percentage elongation, respectively. The outcomes depict that the fibers got stronger and more rigid after treatment. Fiber exposed to a 5% NH solution for 2 h yielded a result comparable to that of fiber treated with a 0.5% NH solution. In all the cases, as the duration of treatment increased from 2 h to 24 h, the fiber degradation increased, which resulted in poor strength. Fiber treated with 10% NH exhibited significantly reduced strength. However, they led to increased elongation. 10%-2-hour fiber exhibited a tensile strength of 244.137 MPa, whereas the fiber treated with the same concentration for 24 h showed the lowest tensile strength of 160.415 MPa. Results show that increased alkali concentration led to excessive fiber degradation. The observed degradation of sisal fibers can be due to the significant elimination of lignin and the breakdown of the structured cellulose chains in the fibers, resulting from prolonged exposure to potent NH solutions [68].

A similar trend was obtained from Figures 9 and 10. Figure 9 denotes the load-displacement curve. The provided statement elucidates the interrelation between the imposed force and the consequent displacement of a substance when exposed to either tension or compression. The test demonstrates the force needed to distort the material to a specific extent and the energy absorbed by the material in the process. The fiber treated for 2 hours with a 0.5% solution showed improved performance. The 10%-2h treated fiber showed greater displacement than the untreated fiber. A 0.5%-2-h fiber supported a load of 11.22 N. With increased duration and concentration of treatment, the load-carrying capacity of the fiber decreased. A modest load caused a significant

displacement. 5%-2 h fibers could take a load of 9.02 N. The load-carrying capacity of untreated fibers was higher than that of fibers treated with a 10% NH solution, which shows that excess concentrations lead to the weakening of fiber structure. Raw fiber could take a load of 5.67N, whereas the load-carrying capacity of 10 hours treated fiber was in the range of 2.7 to 3.17N.

**Table 5:** Tensile strength of fibers.

Sl No	Sample	Tensile Strength (MPa)	Young's Modulus (MPa)	Elongation (%)
1	0.5% -2h	375.679	66.45	9.82
2	0.5% -24h	324.277	31.77	10.14
3	5% -2h	348.219	43	13.3
4	5% -24h	222.04	31	7.23
5	10%-2h	244.137	25.92	9.3
6	10%-24h	160.415	17.28	9.22
7	Raw	194.421	20.19	9.69

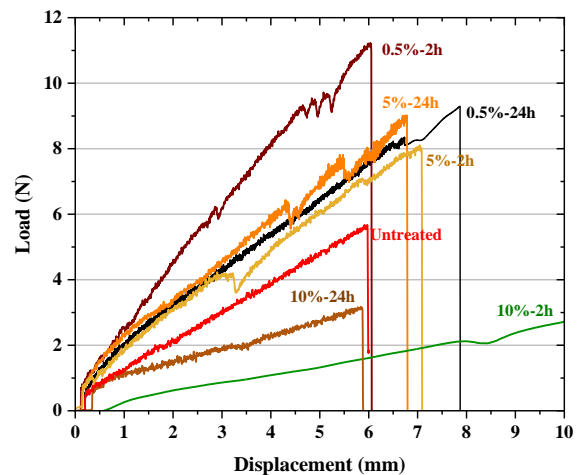


**Figure 9:** Load displacement curve for fiber.

Figure 10 displays the stress-strain curve comparing sisal fiber that has been treated and untreated. The graph indicates that fibers treated with 0.5% NH for 2 h shown greater elasticity compared to the rest. The area under the curve for the fiber treated with 0.5% for 2 h was greater than the others, suggesting it possesses higher toughness.

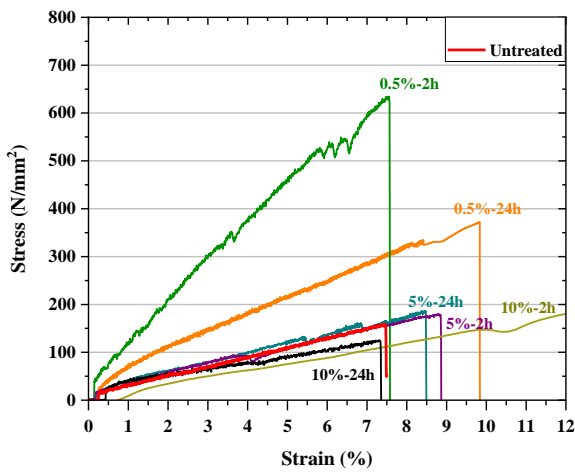


Figure 10: Stress strain curve for fiber.

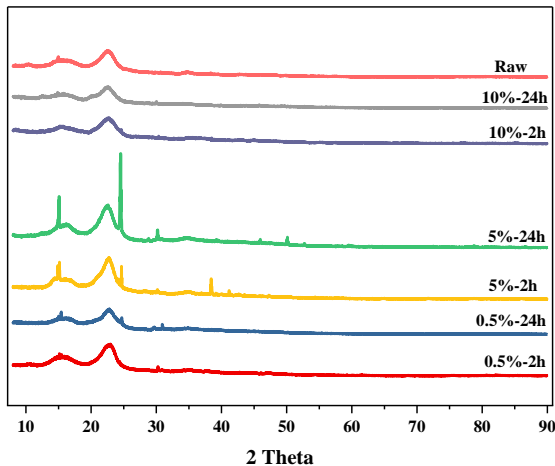


Figure 11: XRD diagram.

### 3.3 XRD analysis

XRD analysis was done to identify the impact of treatment on microstructure and is depicted in Figure 11. The graph exhibited two prominent peaks within the interval of 15 degrees and 22 degrees, which formed due to the reflection of cellulose structures. Fiber treated with 5% NH for 24 h resulted in maximum crystallinity. An increase in the concentration of NH caused higher intensity peaks in the XRD diagram, indicating a greater level of particle organization. However, as the concentration reached 10%, the fiber's crystallinity decreased and became comparable to that of untreated fibers. 10% concentration of alkali caused excessive fiber degradation, resulting in a weaker microstructure than the untreated one. Similar

results were reported by Oushabi *et al.*, [69]. Enhanced crystallinity signifies a higher level of cellulose crystal alignment with the fiber axis after treatments, in comparison to untreated fibers [70]. Following the alkali treatment, the cellulose in the sisal fibers transforms into alkali cellulose. Only the amount of alkali and the treatment methods determine the growth of alkali cellulose [71].

Table 6 shows the crystallinity index of treated and untreated fiber. Fiber treated with 5% NH for 24 h resulted in a maximum crystallinity of 97.7%. Lowest crystallinity was attributed to fibers subjected to 10% NH for 24 h. The crystallinity index for raw fiber was 94.79%. The treatment could lead to a 3.06% enhancement in the crystallinity of fibers. Increased crystallinity index correlates with enhanced fiber stiffness and strength [72]. A rise in the concentration of NH led to a noticeable reduction in crystallinity.

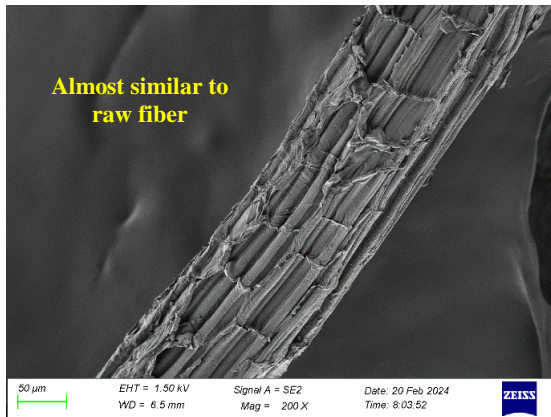
Table 6: Crystallinity index.

Sample	$I_{cr}$	$I_{am}$	Crystallinity Index (%)
0.5%-2h	2907	113	96.11
0.5%-24h	2388	146	93.89
5%-2h	3732	124	96.68
5%-24h	8443	194	97.70
10%-2h	2388	139	94.18
10%-24h	1966	142	92.78
Raw	2401	125	94.79

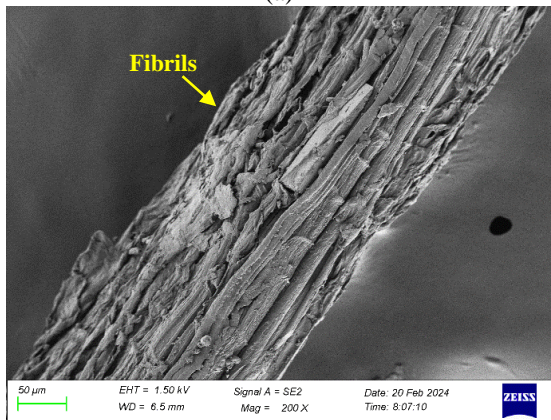
### 3.4 SEM Analysis

Utilising SEM is an efficient way for examining the structure of fibers. Figure 12 displays SEM images of fibers both prior to and post-treatment with different alkali concentrations and durations. Figures 12(a) to 12(c) show the microstructure of fibers treated at 0.5%-2h, 5%-2h, and 10%-2h, respectively. Additionally, the SEM image corresponding to the 10% NaOH treatment for 24 h (Figure 12(d)) is included to illustrate the extreme morphological degradation of the fiber surface under prolonged and aggressive chemical exposure. Figure 12(e) depicts an untreated fiber. As per the findings of a study by Cao *et al.*, fibrillation, or the splitting of packed, untreated fiber, is caused by alkali treatment. Hemicellulose dissolves as a result of fibrillation, which also improves the fiber's surface area [58]. The SEM image reveals that NH-treated fibers have a split of fiber bundles into finer fibrils, but untreated sisal fiber does not exhibit any fibrils. Fibrils were not formed on

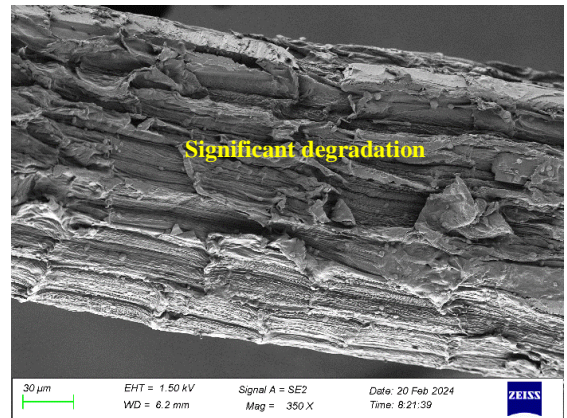
fibers treated with a 0.5% NH solution. However, the one that was subjected to a 5% NH solution formed fibrils, which improved the composite's qualities. When the NH concentration reached 10%, the fiber surface experienced substantial degradation caused by the corrosive nature of the alkaline solution, resulting in severe delignification. However, when compared with the raw fibers, an alkali treatment of 0.5%-2 h resulted in significant removal of contaminants and impurities on the fiber surface.



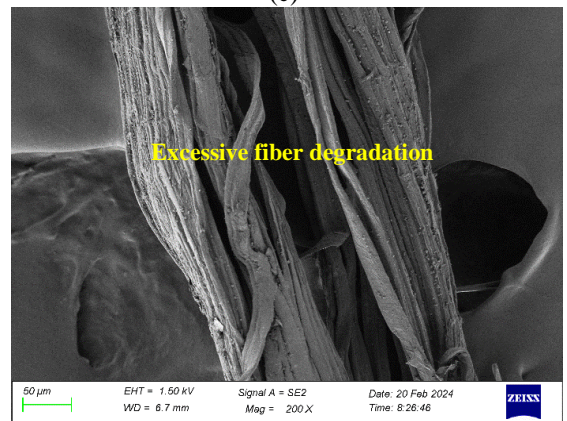
(a)



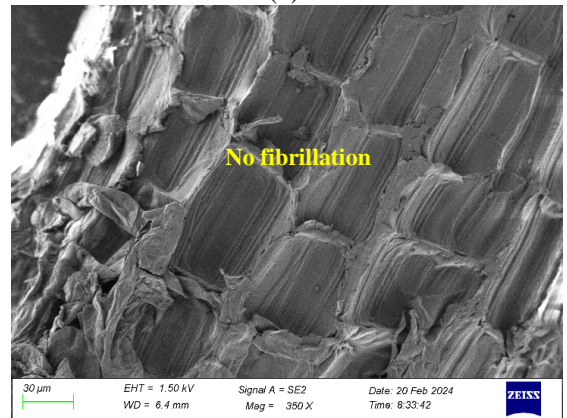
(b)



(c)



(d)

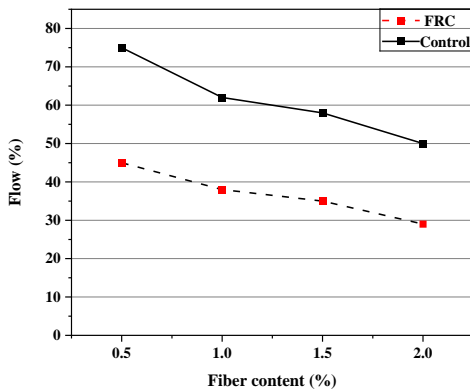


(e)

**Figure 12:** SEM image for (a) 0.5%-2h (b) 5%-2h (c) 10%-2h (d) 10%-24 h and (e) untreated fiber

### 3.5 Workability

The workability of fresh mortar is a critical parameter in fiber-reinforced geopolymer systems, as the inclusion of fibers alters the flowability, viscosity, and compaction behavior of the mix. Therefore, a workability assessment was conducted to ensure that the mechanical and durability enhancements achieved through fiber reinforcement are accompanied by acceptable fresh-state properties for practical applications.



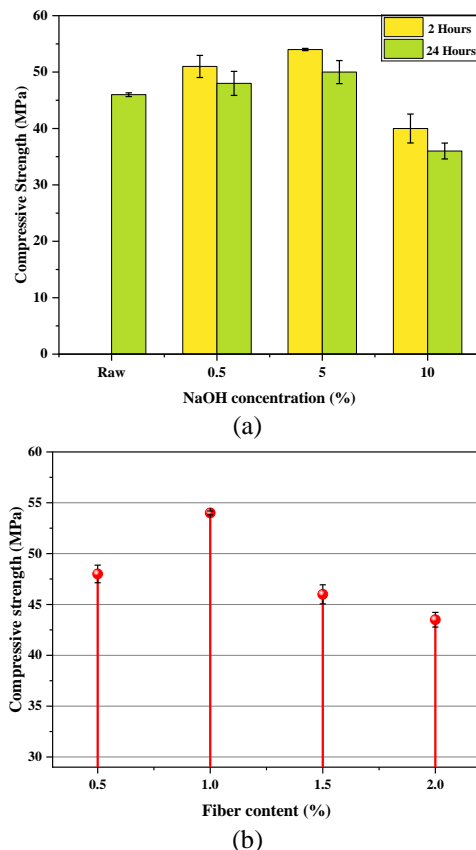
**Figure 13:** Effect of fiber content on workability.

Figure 13 represents the role of fiber in the flow values of mixes. The flow values of fiber reinforced mixes were in the range of 30–45% whereas the flow values of mixes without fiber were between 55–76%. A higher fiber content led to a decrease in the flow of fresh mortar because of the rough surface and uneven distribution of fibers [73]. Exceeding a fiber content of 1% led to a reduction in workability. Pu *et al.*, analyzed that a rise in fiber content reduces flowability because of surface roughness and internal resistance from the fibers. Deng *et al.*, observed similar results where including PVA fibers into the GP mortar resulted in increased viscosity, mostly attributed to the hydrophilic properties and elongated shape of the fibers [74].

### 3.6 CS, FS and STS

The compressive, flexural, and STS of the GP mortar reinforced with sisal fibers are represented in Figures 14–16, respectively. Three specimens were tested for each mix and the average was taken. The results consistently indicated that the inclusion of fiber to the matrix led to enhanced strength qualities. Specifically, implementing treatment measures could enhance the overall performance of the matrix. Moreover, the

findings from all the conducted studies firmly indicate that the alkali content, duration of exposure, and fiber content exert a substantial impact on the efficacy of geopolymer mortar. Figure 14(a) illustrates the CS on 28<sup>th</sup> day with respect to the alkali concentration. Specimens without fiber yielded a CS of 46 MPa on the 28<sup>th</sup> day. The fibers soaked in a 5% solution for a duration of 2 h achieved the highest CS, measuring 54 MPa. Fibers treated with 0.5% NH for 2 h resulted in a strength of 51 MPa, which is close to the highest value. The CS exhibited a negative correlation with both the duration and concentration of the treatment. The fibers exposed to a 10% NH solution for 24 h achieved the lowest strength, measuring at 38 MPa. On the 28<sup>th</sup> day, the implementation of alkali treatment led to a significant 15% increase in CS relative to the untreated fiber combinations. The augmentation of alkali treatment duration and concentration has led to the development of pores within the microstructure of fibers, thereby causing a decline in their load-bearing ability.



**Figure 14:** (a) effect of treatment on CS, (b) effect of fiber content on CS.

FS and STS exhibited a comparable pattern. A FS of 7.4 MPa and STS of 4.69 MPa were observed in the unreinforced specimen. The maximum STS and FS values that were recorded were 5.88 and 8.62 MPa, respectively. Incorporating treated fibers has led to an increase in both flexural and STS. Because the application of NH treatment has enhanced the TS and modulus of elasticity of the fibers. Indeed, the fiber has undergone an increase in rigidity and strength [75]. The enhanced rigidity facilitated the fibers in bearing a greater amount of weight. Furthermore, the implementation of alkali treatment resulted in the generation of fibrils, thus resulting in a rise in the surface area of the fiber. When fibers with a larger surface area came into contact with the mortar, the load-bearing strength of the matrix increased.

When conducting the tensile strength test on single-stranded fiber, fibers that were treated with a 0.5% NH solution for 2 h yielded a superior result. Nevertheless, regarding the mechanical properties, the matrix that contained fibers treated with a 5% NH solution for 2 h yielded superior outcomes. The enhanced characteristics of composites are attributed to the fibrillation of fibers. The SEM analysis confirms that fibrillation has developed in the fibers treated with a concentration of 5% for a duration of 2 h.

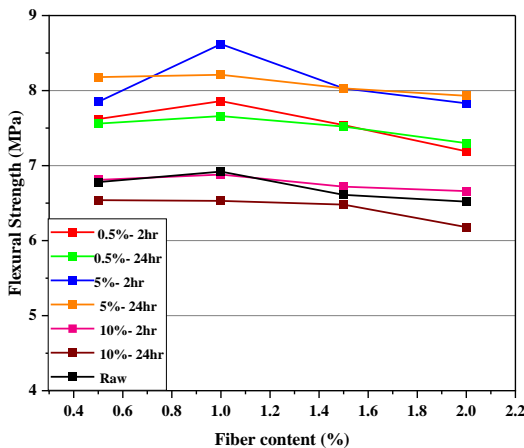


Figure 15: Flexural strength.

Fibers soaked in a 5% NH solution for 24 h showed the highest level of crystallinity when XRD examination was performed on both treated and untreated fibers. However, the increased crystallinity of those fibers rendered them brittle rather than ductile, therefore, they were unable to withstand more load [76]. As a result, the fibers failed to withstand the

strains and broke down, resulting in inadequate results in mechanical strength testing.

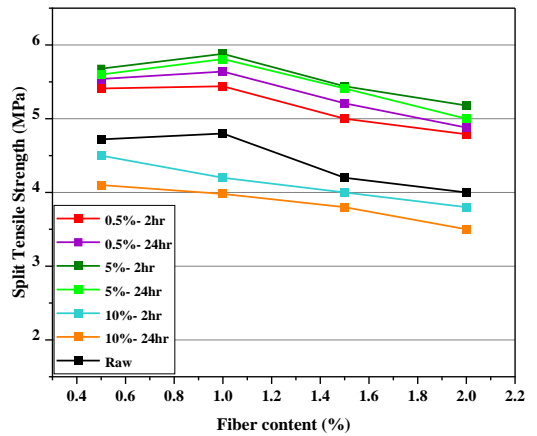


Figure 16: Split tensile strength.

The role of fiber content on the CS, FS, and STS of geopolymer mortar is depicted in Figures 14(b), 15, and 16. The rise in fiber content has resulted in enhanced strength. Tests were performed on specimens with varying fiber volumes, including 0.5, 1, 1.5, and 2%. The specimens exhibited noticeable increases in their CS, FS, and STS with a rise in fiber content from 0.5% to 1%. When the content of fiber exceeded 1%, the strength decreased. As fiber volume increased, the overall density decreased. At higher fiber content, arranging the matrix becomes more difficult, increasing the porosity of the sample. Consequently, there is a reduction in strength [77].

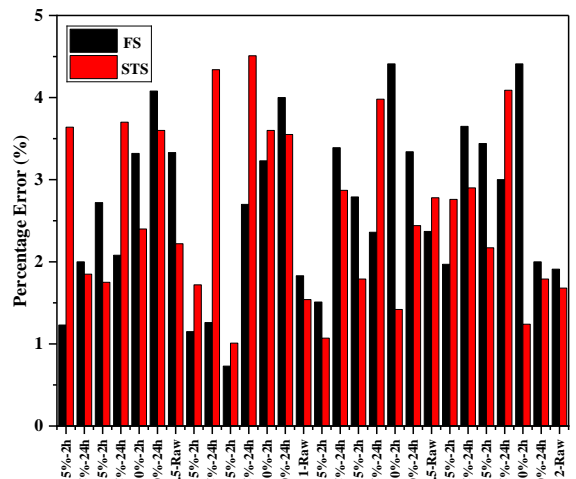


Figure 17: Percentage error of FS and STS.

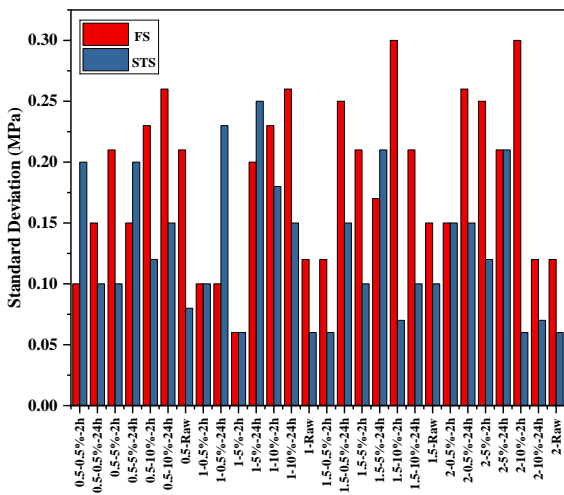


Figure 18: Standard deviation of FS and STS.

The variability analysis of the flexural and split tensile strength results is shown in Figures 17 and 18. The notation given in the X axis consists of three parts. The first part denotes the fiber content (0.5%, 1%, 1.5% and 2%), the second part denotes the NaOH concentration (0.5%, 5% and 10%) and the last part shows the treatment time (2 h and 24 h). The result reveals that the experimental data exhibit excellent consistency across all tested specimens. The standard deviation values for CS varied between 0.1 MPa to 0.43 MPa, FS between 0.06 MPa and 0.30 MPa, and STS varied from 0.06 MPa to 0.25 MPa. Correspondingly, the percentage errors remained relatively low, with most values falling below 4%. This demonstrates the high reliability and repeatability of the mechanical strength measurements performed in this study. It is noteworthy that slightly higher percentage errors, up to approximately 4.5%, were observed in some cases, particularly for higher fiber contents and longer treatment durations. This can be attributed to the natural variability inherent in fiber distribution, fiber-matrix interaction, and possible agglomeration at elevated fiber volumes. Overall, the low standard deviations and percentage errors validate the robustness of the experimental methodology and confirm that the observed trends in mechanical performance are statistically meaningful and not influenced by random errors.

### 3.7 Ultrasonic pulse velocity

The value of the UPV with fiber content is shown in Figure 19. The presence of fibers could change the

outcome since ultrasonic vibrations move through fibers more quickly than they do through mortar. The ultrasonic pulse velocity of mortar strengthened with sisal fiber ranged from 3745 to 4776 m/s. The unreinforced specimen resulted in a pulse velocity of 3997 m/s. The concentration of alkali, duration of treatment, and volume of the fibers have a profound effect on the UPV measurements of the mortar specimens. As the concentration of alkali grew from 0.5% to 5%, the fibers became denser, leading to a higher wave velocity. Nevertheless, upon increasing the alkali concentration to 10%, notable fissures and cavities were noted on the fiber's surface. The introduction of supplementary empty spaces inside the matrix caused a drop in the velocity of the waves [78].

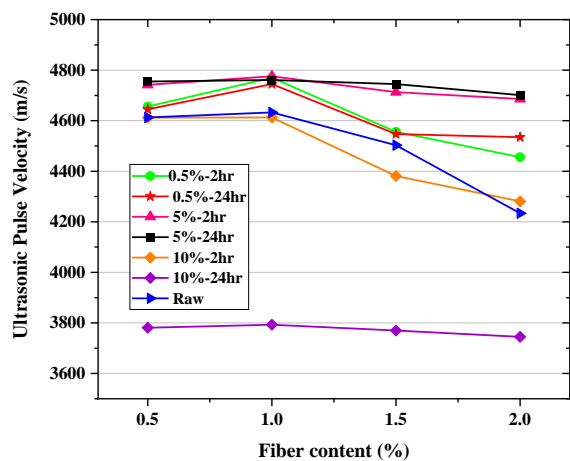


Figure 19: Ultrasonic pulse velocity.

The fiber content is also a crucial aspect of determining the UPV values of GP specimens. The wave velocity was measured for specimens containing varying amounts of fibers, specifically 0.5%, 1%, 1.5%, and 2%. As the fiber proportion went up from 0.5% to 1%, a related rise in the UPV value was observed. The reason for this is that ultrasonic pulses can propagate at a higher velocity through fibers compared to mortar. As the quantity of fibers increased, the speed of the wave likewise increased [79]. Increasing the volume of fiber further led to a decrease in the UPV readings. As the fiber volume exceeded 1%, the density of the mixture decreased. This hindered the propagation of the ultrasonic pulse through the matrix [80].

### 3.8 Water absorption

Figure 20 depicts the water absorption of sisal fiber reinforced OP-GPM. Unreinforced specimens resulted in a water absorption of 15.2%. The incorporation of fibers resulted in significant alterations in water absorption in comparison to the specimens without fibers. The incorporation of fibers subjected to a 0.5% NH treatment for durations of 2 h and 24 h led to a rise in water absorption. The efficacy of the 0.5% alkali treatment in eliminating the hydrophilic chemicals present in the sisal fiber was found to be inadequate. The augmentation of alkali content led to a fall in water absorption as a consequence of the elimination of hydrophilic constituents from the fiber. The highest decrease in water absorption was seen while using a 10% concentration of NH. The time of the treatment process also significantly influences the water absorption characteristics of the composite material. Results have demonstrated that an extended duration of treatment yields greater efficacy. Raising the fiber level from 0.5 to 2% led to a greater amount of water being absorbed. The augmentation in fiber content led to the development of pores through the bond between the fiber and the matrix, thereby promoting improved water absorption [81], [82].

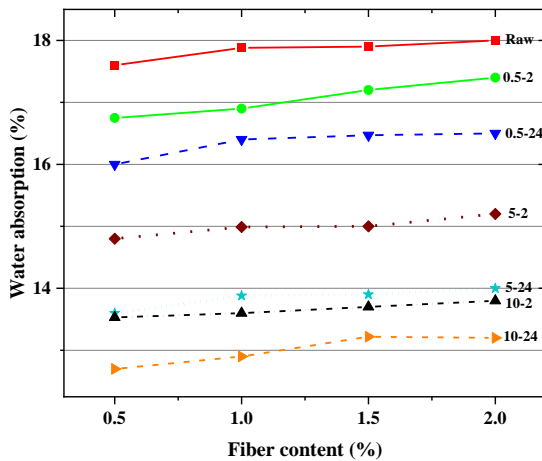


Figure 20: Water absorption of geopolymer mortar.

### 3.9 Acid and sulphate resistance

GP specimens containing 1% fiber were subjected to an acid and sulphate resistance test. The weight loss and CS loss were noted following a 56-day period of exposure to a 5% hydrochloric acid (HCl) and

magnesium sulphate solution for acid and sulphate resistance, respectively. Table 7 shows the test results. The role of alkali treatment in the chemical resistance of fiber-reinforced GP mortars has proven to be considerable. The surface characteristics of fibers are altered by alkali treatment, resulting in enhanced reactivity and stronger bonding with the geopolymer matrix. The improved interfacial bonding decreases the likelihood of fiber withdrawal or separation when exposed to acid, therefore enhancing the overall resilience of the fiber-reinforced composite. Moreover, the augmentation of interaction within the geopolymer matrix results in a reduction in porosity and chemical absorption. Applying alkali treatment can provide alkali resistance to the fibers, hence decreasing their susceptibility to degradation in alkaline environments. The significance of this matter is particularly pronounced in GPC, given its elevated pH conditions. Alkali-resistant fibers exhibit enhanced mechanical qualities and reinforcing capabilities, even when exposed to harsh chemical environments, such as acidic solutions.

Table 7: Acid and sulphate resistance.

NH %	Time (h)	Acid Resistance		Sulphate Resistance	
		Weight Loss (%)	Strength Reduction (%)	Weight Loss (%)	Strength Loss (%)
0.5	2	4.84	8.73	3.01	3.71
	24	6.34	15.49	2.9	4.81
5	2	2.7	3.66	1.12	3.41
	24	2.41	8.15	1.98	6.31
10	2	1.78	13.57	0.89	5.32
	24	1.85	6.2	2.15	4.2
Raw	--	4.71	4.4	3.22	4.33
Unreinforced	--	3.88	5.5	2.02	4.3

### 3.10 Forecasting mechanical properties

Consequently, the experimental data were examined by correlation analysis utilizing Origin software to investigate the correlation among CS, FS, and STS.

#### 3.10.1 Relation between CS and FS

Figure 21 depicts the correlation model between the CS and FS of sisal fiber-reinforced OP-GPM. Equation 3 for the model is given below:

$$Y = 0.0598x + 2.009 \tag{3}$$

Where, Y denotes FS and x represents CS.

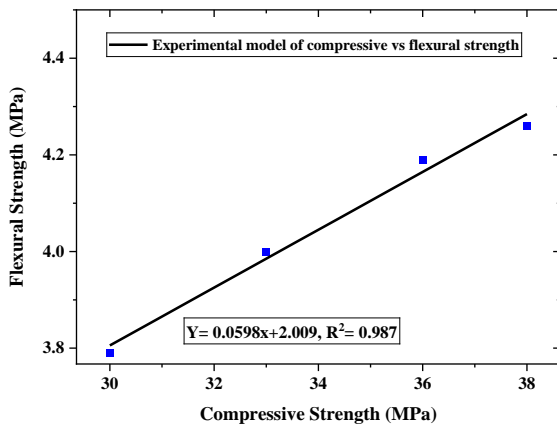


**Figure 21:** Correlation between FS and CS.

The  $R^2$  value was obtained as 0.987. The higher  $R^2$  value signifies that the model accounts for a greater proportion of the variability.

### 3.10.2 Relation between CS and STS

Figure 22 shows the correlation model between the CS and STS of OP-GPM reinforced with sisal fiber. Equation 4 for the model is as follows:

$$Y = 0.037x + 2.204 \quad (4)$$

Where, Y denotes STS and x represents CS.

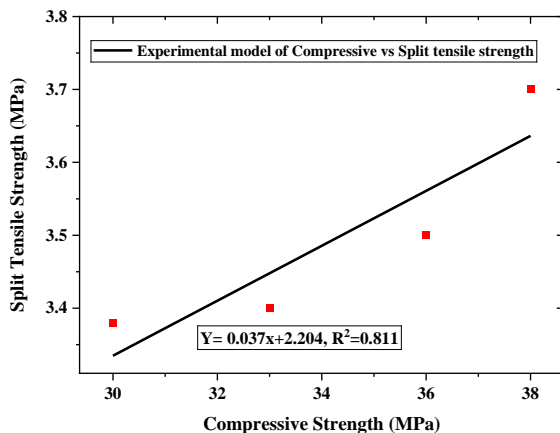


**Figure 22:** Correlation between STS and CS.

The  $R^2$  value obtained was 0.811. In regression analysis, the R-squared value indicates the extent to which the changes in the dependent variable can be attributed to the independent variables. This reflects the level of fit between the regression model and the

observed data. Compared to the CS and FS model, the regression model for CS and STS shows a lower  $R^2$  value. However, with a value of 0.811, the model is closer to 1, implying that it can effectively predict the connection between the dependent and independent variables.

## 4 Conclusions

This study assessed the impact of alkali-treated sisal fiber on the mechanical and durability properties of one-part geopolymer mortar incorporating diatomite, feldspar, and GGBS. Alkali treatment significantly reduced the water absorption of fibers, achieving a 208% reduction compared to untreated fibers, and enhanced fiber tensile strength, with a 134% increase after 0.5% NaOH treatment for 2 h. XRD analysis revealed improved fiber crystallinity, with a maximum increase for fibers treated with 5% NaOH for 24 h. Incorporation of fibers enhanced compressive, flexural, and split tensile strengths, with the best results at 1% fiber content and 5% NaOH treatment for 2 h, achieving compressive strength of 54 MPa, flexural strength of 8.62 MPa, and split tensile strength of 5.88 MPa. Higher fiber volumes (>1%) reduced workability and strength due to poor dispersion. Alkali-treated fibers also improved ultrasonic pulse velocity and chemical resistance against acid and sulphate attack, with notable reductions in weight and strength loss. Regression analysis confirmed strong correlations between compressive strength and other mechanical properties. Overall, the optimal combination of fiber content and treatment effectively improved the performance of the one-part geopolymer mortar, demonstrating its potential as a sustainable construction material.

## Acknowledgment

Funding received from DST SERB Ramanujan fellowship is acknowledged.

## Author contributions

E.S.P.: Conceptualization, Investigation, Methodology, Writing-original draft; P.N.: Supervision, review and editing; J.S.: Supervision, review and editing; B.S.T.: Supervision, review and editing; S.M.K.: Methodology, Investigation; A.T.M.: Methodology, Investigation.

## Conflicts of Interest

The authors declare no conflict of interest.

## References

- [1] E. S. Poojalakshmi, J. Patel, B. Sunantha, B. S. Thomas, K. P. Ramaswamy, and R. Ahmad Khan, "Effect of mechanical activation on the properties of rice husk ash-based one part geopolimer," *Materials Today: Proceedings*, Apr. 2023, doi: 10.1016/j.matpr.2023.04.306.
- [2] D. Khale and R. Chaudhary, "Mechanism of geopolimerization and factors influencing its development: A review," *Journal of Materials Science*, vol. 42, no. 3, pp. 729–746, Feb. 2007, doi: 10.1007/s10853-006-0401-4.
- [3] M. Tuyan, Ö. Andiç-Çakir, and K. Ramyar, "Effect of alkali activator concentration and curing condition on strength and microstructure of waste clay brick powder-based geopolimer," *Composites Part B: Engineering*, vol. 135, pp. 242–252, Feb. 2018, doi: 10.1016/j.compositesb.2017.10.013.
- [4] K. Arunkumar, M. Muthukannan, A. S. Kumar, A. C. Ganesh, and R. K. Devi, "Cleaner environment approach by the utilization of low calcium wood ash in geopolimer concrete," *Applied Science and Engineering Progress*, vol. 15, no. 1, 2022, Art. no. 5165, doi: 10.14416/j.asep.2021.06.005.
- [5] A. Petcherdchoo, T. Hongubon, N. Thanasisathit, K. Punthutaecha, and S. H. Jang, "Effect of curing time on bond strength between reinforcement and fly-ash geopolimer concrete," *Applied Science and Engineering Progress*, vol. 13, no. 2, pp. 127–135, Jun. 2020, doi: 10.14416/j.asep.2020.03.006.
- [6] D. Hardjito, S. E. Wallah, D. M. J. Sumajouw, and B. V. Rangan, "Fly ash-based geopolimer concrete," *Australian Journal of Structural Engineering*, vol. 6, no. 1, pp. 77–86, Sep. 2015, doi: 10.1080/13287982.2005.11464946.
- [7] Z. Li and S. Li, "Effects of wetting and drying on alkalinity and strength of fly ash/slag-activated materials," *Construction and Building Materials*, vol. 254, p. 119069, Sep. 2020, doi: 10.1016/j.conbuildmat.2020.119069.
- [8] M. Mudgal, R. K. Chouhan, S. Kushwah, and A. K. Srivastava, "Enhancing the reactivity and properties of fly ash based solid form geopolimer through ball-milling," *Emerging Materials Research*, vol. 9, no. 1, pp. 1–6, Mar. 2020, doi: 10.1680/jemmr.19.00065.
- [9] I. Faridmehr, M. A. Sahraei, M. L. Nehdi, and K. A. Valerievich, "Optimization of fly ash—slag one-part geopolimers with improved properties," *Materials*, vol. 16, no. 6, p. 2348, Mar. 2023, doi: 10.3390/ma16062348.
- [10] N. Singh, "Fly ash-based geopolimer binder: A future construction material," *Minerals*, vol. 8, no. 7, p. 299, Jul. 2018, doi: 10.3390/min8070299.
- [11] F. Pacheco-Torgal, D. Moura, Y. Ding, and S. Jalali, "Composition, strength and workability of alkali-activated metakaolin based mortars," *Construction and Building Materials*, vol. 25, no. 9, pp. 3732–3745, Sep. 2011, doi: 10.1016/j.conbuildmat.2011.04.017.
- [12] J. Ren, H. Sun, Q. Li, Z. Li, L. Ling, X. Zhang, Y. Wang, and F. Xing, "Experimental comparisons between one-part and normal (two-part) alkali-activated slag binders," *Construction and Building Materials*, vol. 309, Nov. 2021, Art. no. 125177, doi: 10.1016/j.conbuildmat.2021.125177.
- [13] Y. H. M. Amran, R. Alyousef, H. Alabduljabbar, and M. El-Zeadani, "Clean production and properties of geopolimer concrete; A review," *Journal of Cleaner Production*, vol. 251, Apr. 2020, Art. no. 119679, doi: 10.1016/j.jclepro.2019.119679.
- [14] A. Wongsa, R. Kunthawatwong, S. Naenudon, V. Sata, and P. Chindaprasirt, "Natural fiber reinforced high calcium fly ash geopolimer mortar," *Construction and Building Materials*, vol. 241, Apr. 2020, Art. no. 118143, doi: 10.1016/j.conbuildmat.2020.118143.
- [15] Z. Deng, S. Zhang, and Z. Deng, "PVA fiber-reinforced geopolimer mortar made with hybrid recycled aggregates: Toward thermal insulation, lightweight and improved durability," *Journal of Cleaner Production*, vol. 426, Nov. 2023, Art. no. 139200, doi: 10.1016/j.jclepro.2023.139200.
- [16] J. Ayawanna and A. Poowancum, "Enhancing flexural strength of metakaolin-based geopolimer reinforced with different types of fibers," *Sustainable Chemistry and Pharmacy*, vol. 37, Feb. 2024, Art. no. 101439, doi: 10.1016/j.scp.2024.101439.

- [17] M. G. Sá Ribeiro, I. P. A. Miranda, W. M. Kriven, A. Ozer, and R. A. Sá Ribeiro, "High strength and low water absorption of bamboo fiber-reinforced geopolymer composites," *Construction and Building Materials*, vol. 411, Jan. 2024, Art. no. 134179, doi: 10.1016/j.conbuildmat.2023.134179.
- [18] A. Suwansaard, T. Kongpun, and M. Khemkhao, "Properties of mortars mixed with polystyrene and hemp fiber wastes," *Applied Science and Engineering Progress*, vol. 15, no. 1, 2022, Art. no. 5405, doi: 10.14416/j.asep.2021.09.004.
- [19] M. Rajendran, K. Bakthavatchalam, and S. M. Leela Bharathi, "Review on the hybridized application of natural fiber in the development of geopolymer concrete," *Journal of Natural Fibers*, vol. 20, no. 1, Apr. 2023, doi: 10.1080/15440478.2023.2178578.
- [20] K. Korniejenko, E. Frączek, E. Pytlak, and M. Adamski, "Mechanical properties of geopolymer composites reinforced with natural fibers," *Procedia Engineering*, vol. 151, pp. 388–393, 2016, doi: 10.1016/j.proeng.2016.07.395.
- [21] M. Ali, A. Liu, H. Sou, and N. Chouw, "Mechanical and dynamic properties of coconut fibre reinforced concrete," *Construction and Building Materials*, vol. 30, pp. 814–825, May 2012, doi: 10.1016/j.conbuildmat.2011.12.068.
- [22] O. Onuaguluchi and N. Banthia, "Plant-based natural fibre reinforced cement composites: A review," *Cement and Concrete Composites*, vol. 68, pp. 96–108, Apr. 2016, doi: 10.1016/j.cemconcomp.2016.02.014.
- [23] R. D. Tolêdo Filho, K. Scrivener, G. L. England, and K. Ghavami, "Durability of alkali-sensitive sisal and coconut fibres in cement mortar composites," *Cement and Concrete Composites*, vol. 22, no. 2, pp. 127–143, Apr. 2000, doi: 10.1016/S0958-9465(99)00039-6.
- [24] H. Savastano, P. G. Warden, and R. S. P. Coutts, "Microstructure and mechanical properties of waste fibre–cement composites," *Cement and Concrete Composites*, vol. 27, no. 5, pp. 583–592, May 2005, doi: 10.1016/j.cemconcomp.2004.09.009.
- [25] K. Walbrück, F. Maeting, S. Witzleben, and D. Stephan, "Natural fiber-stabilized geopolymer foams—A review," *Materials*, vol. 13, no. 14, p. 3198, Jul. 2020, doi: 10.3390/ma13143198.
- [26] R. Phiri, S. M. Rangappa, S. Siengchin, and D. Marinkovic, "Agro-waste natural fiber sample preparation techniques for bio-composites development: Methodological insights," *Facta Universitatis, Series: Mechanical Engineering*, vol. 21, no. 4, p. 631, Dec. 2023, doi: 10.22190/FUME230905046P.
- [27] S. K. Palaniappan, M. K. Singh, S. M. Rangappa, and S. Siengchin, "Eco-friendly Biocomposites: A step towards achieving sustainable development goals," *Applied Science and Engineering Progress*, vol. 17, no. 4, Feb. 2024, Art. no. 7373, doi: 10.14416/j.asep.2024.02.003.
- [28] J. Wei and C. Meyer, "Degradation mechanisms of natural fiber in the matrix of cement composites," *Cement and Concrete Research*, vol. 73, pp. 1–16, Jul. 2015, doi: 10.1016/j.cemconres.2015.02.019.
- [29] A. M. M. Edeerozey, H. M. Akil, A. B. Azhar, and M. I. Z. Ariffin, "Chemical modification of kenaf fibers," *Materials Letters*, vol. 61, no. 10, pp. 2023–2025, Apr. 2007, doi: 10.1016/j.matlet.2006.08.006.
- [30] P. Sahu and M. Gupta, "A review on the properties of natural fibres and its bio-composites: Effect of alkali treatment," *Proceedings of the Institution of Mechanical Engineers, Part L: Journal of Materials: Design and Applications*, vol. 234, no. 1, pp. 198–217, Jan. 2020, doi: 10.1177/1464420719875163.
- [31] V. Lakshmi Narayana and L. Bhaskara Rao, "A brief review on the effect of alkali treatment on mechanical properties of various natural fiber reinforced polymer composites," *Materials Today Proceedings*, vol. 44, pp. 1988–1994, 2021, doi: 10.1016/j.matpr.2020.12.117.
- [32] L. Y. Mwaikambo and M. P. Ansell, "Chemical modification of hemp, sisal, jute, and kapok fibers by alkalization," *Journal of Applied Polymer Science*, vol. 84, no. 12, pp. 2222–2234, Jun. 2002, doi: 10.1002/app.10460.
- [33] N. Reddy and Y. Yang, "Biofibers from agricultural byproducts for industrial applications," *Trends in Biotechnology*, vol. 23, no. 1, pp. 22–27, Jan. 2005, doi: 10.1016/j.tibtech.2004.11.002.
- [34] M. John and S. Thomas, "Biofibres and biocomposites," *Carbohydrate Polymers*, vol. 71, no. 3, pp. 343–364, Feb. 2008, doi: 10.1016/j.carbpol.2007.05.040.



- [35] N. Reddy and Y. Yang, "Biofibers from agricultural byproducts for industrial applications," *Trends in Biotechnology*, vol. 23, no. 1, pp. 22–27, Jan. 2005, doi: 10.1016/j.tibtech.2004.11.002.
- [36] A. Bledzki, "Composites reinforced with cellulose based fibres," *Progress in Polymer Science*, vol. 24, no. 2, pp. 221–274, May 1999, doi: 10.1016/S0079-6700(98)00018-5.
- [37] L. Yan, N. Chouw, and K. Jayaraman, "Flax fibre and its composites – A review," *Composite B Engineering*, vol. 56, pp. 296–317, Jan. 2014, doi: 10.1016/j.compositesb.2013.08.014.
- [38] A. K. Mohanty, M. Misra, and L. T. Drzal, "Surface modifications of natural fibers and performance of the resulting biocomposites: An overview," *Composite Interfaces*, vol. 8, no. 5, pp. 313–343, Jan. 2001, doi: 10.1163/156855401753255422.
- [39] S. İlkenntapar and A. Özsoy, "Investigation of mechanical properties, high-temperature resistance and microstructural properties of diatomite-containing geopolymer mortars," *Arabian Journal of Geosciences*, vol. 15, no. 6, p. 502, Mar. 2022, doi: 10.1007/s12517-022-09824-7.
- [40] R. C. Abruzzi, B. A. Dedavid, and M. J. R. Pires, "Characterization of tin dioxide nanoparticles synthesized by oxidation," *Cerâmica*, vol. 61, no. 359, pp. 328–333, Sep. 2015, doi: 10.1590/0366-69132015613591919.
- [41] J. J. Kipsanai, P. M. Wambua, S. S. Namango, and S. Amziane, "A review on the incorporation of diatomaceous earth as a geopolymer-based concrete building resource," *Materials*, vol. 15, no. 20, p. 7130, Oct. 2022, doi: 10.3390/ma15207130.
- [42] D. M. González-García, L. Téllez-Jurado, F. J. Jiménez-Álvarez, and H. Balmori-Ramírez, "Structural study of geopolymers obtained from alkali-activated natural pozzolan feldspars," *Ceramics International*, vol. 43, no. 2, pp. 2606–2613, Feb. 2017, doi: 10.1016/j.ceramint.2016.11.070.
- [43] N. T. Abdel-Ghani, H. A. Elsayed, and S. AbdelMoied, "Geopolymer synthesis by the alkali-activation of blastfurnace steel slag and its fire-resistance," *HBRC Journal*, vol. 14, no. 2, pp. 159–164, Aug. 2018, doi: 10.1016/j.hbrj.2016.06.001.
- [44] I. Suyambulingam, S. M. Rangappa, and S. Siengchin, "Advanced materials and technologies for engineering applications," *Applied Science and Engineering Progress*, vol. 16, no. 3, Jan. 2023, Art. no. 6760, doi: 10.14416/j.asep.2023.01.008.
- [45] B. Lavanya, P. D. Kuriya, S. Suganesh, R. Indrajith, and R. B. Chokkalingam, "Properties of geopolymer bricks made with flyash and GGBS," *IOP Conference Series Material Science Engineering*, vol. 872, no. 1, Jun. 2020, Art. no. 012141, doi: 10.1088/1757-899X/872/1/012141.
- [46] A. Saludung, Y. Ogawa, and K. Kawai, "Microstructure and mechanical properties of FA/GGBS-based geopolymer," *MATEC Web of Conferences*, vol. 195, Aug. 2018, Art. no. 01013, doi: 10.1051/mateconf/201819501013.
- [47] H. El-Hassan and N. Ismail, "Effect of process parameters on the performance of fly ash/GGBS blended geopolymer composites," *Journal of Sustainable Cement Based Materials*, vol. 7, no. 2, pp. 122–140, Mar. 2018, doi: 10.1080/21650373.2017.1411296.
- [48] Rao, G. Srinivasa, and B. Sarath Chandra Kumar, "Experimental investigation of GGBS based geopolymer concrete with steel fibers," *International Conference on Advances in Civil Engineering (ICACE-2019)*, vol. 21, p. 23, 2019.
- [49] N. Degirmenci and A. Yilmaz, "Use of diatomite as partial replacement for Portland cement in cement mortars," *Construction and Building Materials*, vol. 23, no. 1, pp. 284–288, Jan. 2009, doi: 10.1016/j.conbuildmat.2007.12.008.
- [50] C. Li, G. Li, D. Chen, K. Gao, Y. Cao, Y. Zhou, Y. Mao, S. Fan, L. Tang, and H. Jia, "The effects of diatomite as an additive on the macroscopic properties and microstructure of concrete," *Materials*, vol. 16, no. 5, p. 1833, Feb. 2023, doi: 10.3390/ma16051833.
- [51] S. S. Ibrahim, "Diatomite ores: Origin, characterization and applications," *Journal of International Environmental Application & Science*, vol. 7, no. 1, pp. 191–199, 2012.
- [52] E. E. ElSayed, "Natural diatomite as an effective adsorbent for heavy metals in water and wastewater treatment (a batch study)," *Water Science*, vol. 32, no. 1, pp. 32–43, Apr. 2018, doi: 10.1016/j.wsj.2018.02.001.

- [53] P. Zhao, N. Sun, X. Liu, Z. Chen, Y. Li, T. Hu, X. Xue, S. Zhang, G. Sheeta, and Y. Xie, "Diatomite-based adsorbent decorated with Fe<sub>3</sub>O<sub>4</sub> nanoparticles for the removal of hazardous metal ions," *ACS Applied Nano Materials*, vol. 6, no. 10, pp. 8958–8970, May 2023, doi: 10.1021/acsnm.3c01577.
- [54] O. Şan and A. İmaretli, "Preparation and filtration testing of diatomite filtering layer by acid leaching," *Ceramics International*, vol. 37, no. 1, pp. 73–78, Jan. 2011, doi: 10.1016/j.ceramint.2010.08.030.
- [55] V. Bhardwaj and M. J. Mirliss, "Diatomaceous earth filtration for drinking water," *National Drinking Water Clearing House Fact Sheet*, vol. 1, no. 4, 2001.
- [56] C. Bağcı, G. P. Kutyla, and W. M. Kriven, "Fully reacted high strength geopolymer made with diatomite as a fumed silica alternative," *Ceramics International*, vol. 43, no. 17, pp. 14784–14790, Dec. 2017, doi: 10.1016/j.ceramint.2017.07.222.
- [57] *Standard Test Method for Tensile Strength and Young's Modulus of Fibers*, ASTM-C1557-03, 2003.
- [58] L. Segal, J. J. Creely, A. E. Martin, and C. M. Conrad, "An empirical method for estimating the degree of crystallinity of native cellulose using the x-ray diffractometer," *Textile Research Journal*, vol. 29, no. 10, pp. 786–794, Oct. 1959, doi: 10.1177/004051755902901003.
- [59] *Standard Test Method for Flow of Hydraulic Cement Mortar*, ASTM C1437-01, 2001
- [60] *Standard Test Method for Compressive Strength of Hydraulic Cement Mortars (Using 2-in. or [50-mm] Cube Specimens)<sup>1</sup>*, ASTM C109/C109M-02, 2002.
- [61] *Standard Test Method for Flexural Strength of Hydraulic-Cement Mortars<sup>1</sup>*, ASTM C348-02, 2002.
- [62] *Standard Test Method for Splitting Tensile Strength of Cylindrical Concrete Specimens*, ASTM C496/C496M-11, 2011.
- [63] *Standard Test Method for Pulse Velocity Through Concrete 1*, ASTM C597-16, 2016.
- [64] *Test Method for Density, Absorption, and Voids in Hardened Concrete*, ASTM C642-13, 2013.
- [65] *Standard Test Methods for Determining the Chemical Resistance of Concrete Products to Acid Attack 1*, ASTM C1898-20, 2020.
- [66] *Standard Test Methods for Chemical Resistance of Mortars, Grouts, and Monolithic Surfacing and Polymer Concretes*, ASTM C267-01, 2001.
- [67] T. Yimer and A. Gebre, "Effect of fiber treatments on the mechanical properties of sisal fiber-reinforced concrete composites," *Advances in Civil Engineering*, vol. 2023, pp. 1–15, Apr. 2023, doi: 10.1155/2023/2293857.
- [68] L. Y. Mwaikambo and M. P. Ansell, "Mechanical properties of alkali treated plant fibres and their potential as reinforcement materials. I. hemp fibres," *Journal of Materials Science*, vol. 41, no. 8, pp. 2483–2496, Apr. 2006, doi: 10.1007/s10853-006-5098-x.
- [69] A. Oushabi, S. Sair, F. O. Hassani, Y. Abboud, O. Tanane, and A. E. Bouari, "The effect of alkali treatment on mechanical, morphological and thermal properties of date palm fibers (DPFs): Study of the interface of DPF–Polyurethane composite," *South African Journal of Chemical Engineering*, vol. 23, pp. 116–123, Jun. 2017, doi: 10.1016/j.sajce.2017.04.005.
- [70] F. J. Kolpak, M. Weih, and J. Blackwell, "Mercerization of cellulose: 1. Determination of the structure of Mercerized cotton," *Polymer (Guildf)*, vol. 19, no. 2, pp. 123–131, Feb. 1978, doi: 10.1016/0032-3861(78)90027-7.
- [71] P. Krishnaiah, C. T. Ratnam, and S. Manickam, "Enhancements in crystallinity, thermal stability, tensile modulus and strength of sisal fibres and their PP composites induced by the synergistic effects of alkali and high intensity ultrasound (HIU) treatments," *Ultrasonics Sonochemistry*, vol. 34, pp. 729–742, Jan. 2017, doi: 10.1016/j.ultsonch.2016.07.008.
- [72] M. Benzerzour, N. Sebaibi, N. E. Abriak, and C. Binetruy, "Waste fibre–cement matrix bond characteristics improved by using silane-treated fibres," *Construction and Building Materials*, vol. 37, pp. 1–6, Dec. 2012, doi: 10.1016/j.conbuildmat.2012.07.024.
- [73] P. Lertwattanaruk and A. Suntijitto, "Properties of natural fiber cement materials containing coconut coir and oil palm fibers for residential building applications," *Construction and Building Materials*, vol. 94, pp. 664–669, Sep. 2015, doi: 10.1016/j.conbuildmat.2015.07.154.
- [74] Z. Deng, Z. Yang, J. Bian, X. Pan, G. Wu, F. Guo, R. Fu, H. Yan, Z. Deng, and S. Chen, "Engineering properties of PVA fibre-

- reinforced geopolymer mortar containing waste oyster shells,” *Materials*, vol. 15, no. 19, p. 7013, Oct. 2022, doi: 10.3390/ma15197013.
- [75] T. Alomayri, F. U. A. Shaikh, and I. M. Low, “Characterisation of cotton fibre-reinforced geopolymer composites,” *Composites Part B: Engineering*, vol. 50, pp. 1–6, Jul. 2013, doi: 10.1016/j.compositesb.2013.01.013.
- [76] M. Y. Hashim, A. M. Amin, O. M. F. Marwah, M. H. Othman, M. R. M. Yunus, and N. Chuan Huat, “The effect of alkali treatment under various conditions on physical properties of kenaf fiber,” *Journal of Physics Conference Series*, vol. 914, Oct. 2017, Art. no. 012030, doi: 10.1088/1742-6596/914/1/012030.
- [77] J. Khedari, B. Suttisonk, N. Pratinthong, and J. Hirunlabh, “New lightweight composite construction materials with low thermal conductivity,” *Cement and Concrete Composites*, vol. 23, no. 1, pp. 65–70, Feb. 2001, doi: 10.1016/S0958-9465(00)00072-X.
- [78] B. Muñoz-Sánchez, M. J. Arévalo-Caballero, and M. C. Pacheco-Menor, “Influence of acetic acid and calcium hydroxide treatments of rubber waste on the properties of rubberized mortars,” *Materials and Structures*, vol. 50, no. 1, p. 75, Feb. 2017, doi: 10.1617/s11527-016-0912-7.
- [79] R. Ghosh, S. P. Sagar, A. Kumar, S. K. Gupta, and S. Kumar, “Estimation of geopolymer concrete strength from ultrasonic pulse velocity (UPV) using high power pulser,” *Journal of Building Engineering*, vol. 16, pp. 39–44, Mar. 2018, doi: 10.1016/j.jobbe.2017.12.009.
- [80] S. Shankar and H. R. Joshi, “Comparison of concrete properties determined by destructive and non-destructive tests,” *Journal of the Institute of Engineering*, vol. 10, no. 1, pp. 130–139, Aug. 2014, doi: 10.3126/jie.v10i1.10889.
- [81] D. M. Ali, S. C. Chin, C. Bao, and J. Gimbun, “Enhancement of reinforced concrete durability and performance by bamboo and basalt fibres,” *Physics and Chemistry of the Earth, Parts A/B/C*, vol. 134, Jun. 2024, Art. no. 103572, doi: 10.1016/j.pce.2024.103572.
- [82] S. Balachandran, J. Sudhakumar, B. S. Thomas, P. Sankaranarayanan, S. T. Vasu, and A. C. Ravikumar, “Mechanical properties of bacterial cement mortar integrating natural banana fibres,” *Applied Science and Engineering Progress*, vol. 17, no. 4, 2024, Art. 7549, doi: 10.14416/j.asep.2024.09.002.